

## ARTICLES

# Ultrafast Infrared Studies of Bond Activation in Organometallic Complexes

HAW YANG, KENNETH T. KOTZ,  
MATTHEW C. ASPLUND,  
MATTHEW J. WILKENS, AND  
CHARLES B. HARRIS\*

*Department of Chemistry, University of California, Berkeley, California 94720, and Chemical Sciences Division, Ernest Orlando Lawrence Berkeley National Laboratory, Berkeley, California 94720*

Received June 1, 1998

## 1. Introduction

The ability to directly monitor the progress of chemical reactions as they take place is one of the major recent developments in physical chemistry. Many of the advances in our understanding of chemical processes have come about as a result of time-resolved spectroscopic techniques. Conventional methods of time resolution, however, are limited to microsecond and slower regimes, curtailing the applicability of such techniques in many cases of interest. Ultrafast spectroscopy, made possible by the invention and subsequent refinement of pulsed laser technology, has become one of the most powerful

tools available to chemists by providing insight into those physical and chemical phenomena which occur too rapidly to be studied by traditional methods. Processes amenable to investigation by ultrafast techniques include electron transfer reactions, vibrational and electronic relaxation in molecules large and small, reaction dynamics in natural and artificial photosynthetic systems, and surface phenomena in both bulk and microscopic systems, to name only a few. Predominate in the field are UV-pump visible-probe techniques, a fact which derives largely from the early development of practical UV and visible sources. UV-vis experiments, widely applied to the study of physical phenomena, convey information about those (primarily electronic) transitions which involve the absorption of visible probe photons. Chemically important information, including structures, can be obtained by examining the IR region of the spectrum, which offers better spectral resolution, a greater number of spectral features, and increased sensitivity to the chemical environment.

One problem which is amenable to study using ultrafast vibrational spectroscopy is bond activation, the weakening of otherwise stable chemical bonds so as to increase their reactivity. This is an area of particular interest to organic chemists since many organic reactions involve breaking the extremely stable (>90 kcal/mol) carbon-hydrogen (C-H) and silicon-hydrogen (Si-H) bonds of alkanes and silanes, respectively. A mild (i.e., room temperature and ambient pressure) path to C-H bond activation is also of obvious interest to the petrochemical industry. Si-H bond activation by certain transition-metal-containing compounds was discovered by Jetz and Graham in 1971.<sup>1</sup> This was followed in 1982 by the discovery of a related activation reaction of alkane C-H bonds involving Cp\*(L)IrH<sub>2</sub> (Cp\* = (CH<sub>3</sub>)<sub>5</sub>C<sub>5</sub>)<sup>2,3</sup> and Cp\*Ir(CO)<sub>2</sub>.<sup>4</sup> Efforts to understand the dynamics of these activation reactions have been made by several groups using gas-phase,<sup>5</sup> low-temperature/high-pressure liquid noble gas,<sup>6,7</sup> or matrix isolation<sup>8–10</sup> experiments. These techniques slow the reactions, thereby rendering the intermediates observable using conventional Fourier transform IR (FTIR), UV-vis, and fluorescence spectroscopies. Though fruitful, these methods share the disadvantage of observing the activation reactions under conditions quite different from those under which they are normally carried out.

Femtosecond infrared spectroscopy provides an ideal tool for investigating the real-time dynamics of these reactions because it provides sufficient temporal resolution to observe all early intermediate steps under ambient reaction conditions. Carbonyl stretches in the 1850–2050 cm<sup>-1</sup> range have large absorption cross sections and display significant shifts (>10 cm<sup>-1</sup>) with changing chemi-

Haw Yang was born in Taichung, Taiwan, in 1969. He received his B.S. degree from National Taiwan University in 1991. He is currently a graduate student at the University of California, Berkeley, under the direction of Charles Harris.

Kenneth T. Kotz was born in Detroit, MI, in 1973. He received his B.S. degree from the University of Michigan in 1995. He is currently a graduate student at the University of California, Berkeley, under the direction of Charles Harris.

Matthew C. Asplund was born in Edmonton, Alberta, Canada, in 1967. He received his B.S. degree from Brigham Young University in 1992 and his Ph.D. in 1998 from the University of California, Berkeley, under the direction of Charles Harris. He is currently a postdoctoral fellow at the University of Pennsylvania under the direction of Robin Hochstrasser.

Matthew J. Wilkens was born in Rochester, NY, in 1974. He received his B.S. degree from the College of William & Mary in 1996 and his M.S. degree from the University of California, Berkeley, in 1998, where he worked under the direction of Charles Harris. He is currently a graduate student at the University of Wisconsin.

Charles B. Harris was born in New York, NY, in 1940. He received his B.S. degree from the University of Michigan in 1963 and his Ph.D. from the Massachusetts Institute of Technology in 1966, under the direction of F. A. Cotton. Following a postdoctoral fellowship in physics from the Atomic Energy Commission at MIT, he joined the faculty at the University of California, Berkeley, in 1967. He currently holds appointments as Professor of Chemistry at UC Berkeley and Principle Investigator, Chemical Sciences Division, Lawrence Berkeley National Laboratory. In addition to his work with organometallic reaction dynamics, his research also focuses on ultrafast electronic phenomena at surfaces and at interfaces.

\* To whom correspondence should be addressed at the University of California.

cal environment, including changes in hapticity, electronic structure, and ligand identity, making them useful spectroscopic probes of chemical reactivity at the metal center. By following changes in these spectroscopic features through time, it is possible not only to identify reaction intermediates but also to correlate the various intermediates to one another. This information can then be used to determine reaction mechanisms, branching ratios, energy barriers, and intermediate structures for each reaction.

$\text{Tp}^*\text{Rh}(\text{CO})_2$  ( $\text{Tp}^* = \text{HB-Pz}^*_3$ ,  $\text{Pz}^* = 3,5\text{-dimethylpyrazolyl}$ ) and  $\text{CpM}(\text{CO})_3$  ( $\text{M} = \text{Mn, Re}$ ) have been used in the current studies of  $\text{C-H}^{12,13}$  and  $\text{Si-H}^{14,15}$  bond activation, respectively. The ultrafast experimental setup has been described in the literature,<sup>16</sup> and will not be presented here. Time-resolved nanosecond step-scan FTIR spectroscopy<sup>17</sup> has been used to follow the dynamics of longer-lived intermediate species. Finally, first principle (ab initio) quantum mechanical calculations have been undertaken to assist in the elucidation of intermediate structures. The specific types and level of calculations carried out in these studies are discussed elsewhere and will not be repeated here (ref 15 and references therein). In general, the calculations support the interpretation of the data presented here within the accuracy of the data and the limitations of the computational methods used.

## 2. Carbon–Hydrogen Bond Activation

Gas-phase spectroscopy of  $\text{CpRh}(\text{CO})_2$ ,<sup>18</sup> in which there are no solvent molecules with which the metal center may react, showed that the first transient product following photoexcitation of  $\text{CpRh}(\text{CO})_2$  is the monocarbonyl  $\text{CpRh}(\text{CO})$ . Research on the same molecule in inert liquid rare gases,<sup>6</sup> where there are some solvent interactions, but where there can be no chemical reactions, shows the prompt formation of a solvent complex. Further studies have shown that, in dilute solutions of alkanes in rare gas liquids, these rare gas molecules can exchange with alkane molecules to form a  $\text{C-H}$ -activated final product. Measurements of the exchange rates give a time for bond activation of  $\sim 2 \mu\text{s}$  at a temperature of 73 K.<sup>7</sup>

An interesting question in understanding and eventually making use of these reactions is what effect those ligands which are coordinated to the metal center have on the quantum yield of the reaction. The quantum yield of  $\text{CpRh}(\text{CO})_2$  is 1%, while the quantum yield of  $\text{Cp}^*\text{Rh}(\text{CO})_2$  ( $\text{Cp}^* = \text{C}_5\text{H}_5$ ;  $\text{Cp}^* = \text{C}_5(\text{CH}_3)_5$ ) is only 0.2%.<sup>19</sup> Thus, a small change in the structure of the ligand can have a significant impact on the reaction yield. This change in yield is important in the reaction, as it will allow for the design of more efficient catalytic systems.

**2.1. Ultrafast Visible Spectroscopy.** It was shown by Bengali et al. and Weiller et al.<sup>6,7,18</sup> that the reactive intermediate in the  $\text{Cp}^*\text{Rh}(\text{CO})_2$  system is a monocarbonyl,  $\text{Cp}^*\text{Rh}(\text{CO})$ . An important issue to be resolved then is the state of the 99% of the molecules which are unreactive. Ultrafast infrared measurements made by Dougherty and Heilweil show that there are no mono-

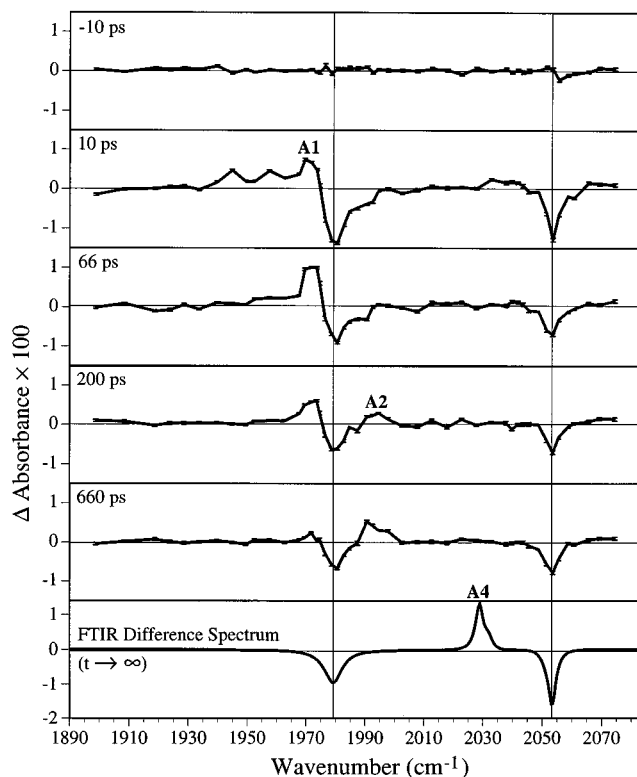


**FIGURE 1.** Time-resolved ultrafast spectra of  $\text{Tp}^*\text{Rh}(\text{CO})_2$  in cyclohexane. The last panel is a static FTIR difference spectrum before and after UV photolysis at 308 nm.

carbonyl peaks in the CO region of the spectra.<sup>20</sup> This suggests that the unreactive molecules are dicarbonyls, indicating that the yield for this reaction is controlled by CO dissociation. All molecules which undergo CO dissociation go on to form alkyl hydride product, and no molecules which do not undergo CO dissociation go on to form product. This means that the quantum yield depends only on the branching ratio of the initial photoexcitation. Ultrafast measurements made by Bromberg et al. and Lian et al.<sup>11</sup> provide additional information. Immediately after photoexcitation, a new species with an electronic transition in the visible region of the spectrum was observed. This species was formed in less than 1 ps, and decays in a biexponential manner. This is assigned to an electronic intermediate state, which decays to the ground electronic state on a time scale of 30–40 ps.

To understand the mechanism of these reactions, it is necessary to study a system in which a larger percentage of excited molecules are in a CO dissociative state. The molecule  $\text{Tp}^*\text{Rh}(\text{CO})_2$ , as studied by Graham, Ghosh, Lees, and Purwoko,<sup>21–24</sup> has a quantum yield of 30%, thereby providing a sufficient concentration of intermediates to measure their structural changes. The  $\text{Tp}^*$  ligand is also thought to have chemistry similar to that of the Cp and  $\text{Cp}^*$  ligands.

**2.2. Ultrafast and Nanosecond IR Spectroscopy.** Figure 1 shows time-resolved IR spectra of  $\text{Tp}^*\text{Rh}(\text{CO})_2$  in cyclohexane from 10 ps before to 660 ps after photoexcitation. At the earliest time after photoinitiation (10 ps) there is a depletion of the parent absorptions at 1980 and 2050  $\text{cm}^{-1}$  and a new series of peaks starting at 1972  $\text{cm}^{-1}$  and

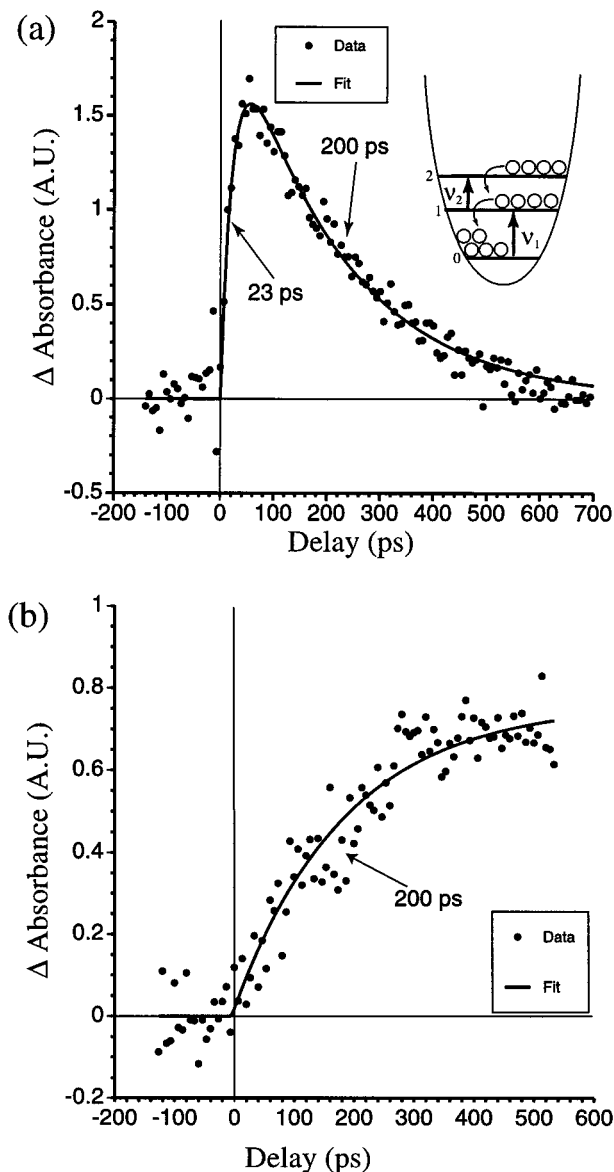


**FIGURE 2.** Ultrafast kinetics of C–H bond activation in *n*-pentane. (a) Intermediate **A1** at  $1972\text{ cm}^{-1}$ . Inset: Schematic depiction of vibrational cooling. As the population shifts to lower vibrational levels, the absorption frequency shifts to higher energy. (b) Intermediate **A2** at  $1990\text{ cm}^{-1}$ .

extending to lower frequencies. The  $1972\text{ cm}^{-1}$  feature is attributed to a monocarbonyl species because there is not a corresponding peak at  $1900$  or  $2040\text{ cm}^{-1}$  as expected and observed in all dicarbonyl species. Previous studies performed on other metal carbonyl systems show that the newly formed unsaturated species forms a weakly bound solvent complex in less than  $2\text{ ps}$ .<sup>25</sup> In light of these studies, it is concluded that the intermediate species **A1** is a monocarbonyl solvent complex. This intermediate has excess vibrational energy from the photoexcitation, as indicated by the excited CO stretches. The solvent complex transfers this vibrational energy to the solvent on a time scale of  $23\text{ ps}$ , as shown in Figure 2a. This is consistent with measurements on other metal carbonyls such as  $\text{CpCo}(\text{CO})_2$ ,<sup>20</sup>  $(\text{acac})\text{Rh}(\text{CO})_2$ <sup>26</sup> ( $\text{acac} = \text{acetyl acetate}$ ),

and  $\text{M}(\text{CO})_6$  ( $\text{M} = \text{Cr, Mo, or W}$ ).<sup>16,27–29</sup> Intermediate **A1** then decays away with a time constant of  $200\text{ ps}$ .

On the same time scale, a new intermediate **A2** grows in with a CO absorption at  $1992\text{ cm}^{-1}$ . This species also contains only one CO stretch, and so is also a monocarbonyl. From the spectral shift of the CO stretch ( $20\text{ cm}^{-1}$  higher in energy) it can be inferred that the electron density on the metal center has decreased. In this case, there is less back-bonding into the antibonding  $\pi^*$  CO molecular orbital, and a correspondingly higher vibrational frequency. Ultrafast measurements show that **A2** persists to  $>1\text{ ns}$ . Nanosecond step-scan measurements in the CO region (Figures 3 and 4) show that, in cyclohexane, the lifetime of **A2** is  $230\text{ ns}$  and that it converts quantitatively to the final C–H-activated product, which has a CO absorption at  $2032\text{ cm}^{-1}$ .

**2.3. Nature of the Alkane Intermediates.** In the dicarbonyl ground state, there is evidence that the  $\eta^3\text{-Tp}^*\text{Rh}(\text{CO})_2$  is in equilibrium with  $\eta^2\text{-Tp}^*\text{Rh}(\text{CO})_2$ , with an equilibrium constant  $K_{\text{eq}} = 100$  favoring the  $\eta^3$  form.<sup>24</sup> This suggests that the  $\text{Tp}^*$  ligand is labile, and can chelate and dechelate the rhodium atom. A similar chemical system, a Pt(IV) compound studied by Wick and Goldberg,<sup>30</sup> provides an interesting comparison in reactivity. In that case, an  $\eta^2\text{-Tp}^*\text{PtMe}_2$  system which shows C–H activation after reaction with  $\text{B}(\text{C}_6\text{F}_5)_3$  was studied. These workers found that they were able to form  $\eta^3\text{-Tp}^*\text{Pt}(\text{Me})(\text{R})(\text{H})$  product, and proposed a dissociative mechanism in which the  $\text{B}(\text{C}_6\text{F}_5)_3$  abstracts a methyl group to give an  $\eta^2\text{-Tp}^*\text{PtMe}$  intermediate species. This species then reacts with a solvent molecule, forming a Pt–N bond with the third pyrazole ring to form the  $\eta^3$  final product.

This suggests a possible identity for intermediate **A2**, a partially dechelated  $\eta^2\text{-Tp}^*\text{Rh}(\text{CO})(\text{S})$  monocarbonyl solvent complex. Although the Rh metal center is already coordinatively unsaturated after dissociation of the CO molecule in the first step of the reaction, density functional ab initio calculations performed by Zaric and Hall<sup>31</sup> show that, for a  $\text{Tp}^*\text{Rh}(\text{CO})(\text{CH}_4)$  complex in the gas phase, the energy of the  $\eta^2$  form is  $9\text{ kcal/mol}$  lower (more stable) than that of the  $\eta^3$  form. Moreover, calculation of the vibrational modes shows that the CO stretching frequency is shifted to higher energy in the  $\eta^2$  form than in the  $\eta^3$  form.

The identity of **A2** can be confirmed through the observation of the closely analogous  $\text{Bp}^*\text{Rh}(\text{CO})_2$  ( $\text{Bp}^* = \text{H}_2\text{B-Pz}^*_2$ ) system. This complex also has an absorption in the near-UV which leads to the dissociation of a CO group and the subsequent formation of a solvent complex. In the ground dicarbonyl state, the CO stretches are shifted  $+30\text{ cm}^{-1}$  to higher energy because of the change in electron density resulting from one fewer Rh–N bond. This shift is similar to the shift between **A1** ( $1972\text{ cm}^{-1}$ ) and **A2** ( $1990\text{ cm}^{-1}$ ). Time-resolved IR measurements show that, following photoexcitation, a CO group is lost and a solvent complex forms with a CO stretching band at  $1990\text{ cm}^{-1}$ , the same frequency as that of intermediate **A2**. This band persists for microseconds, though it is not observed in static measurements, and so must decay away

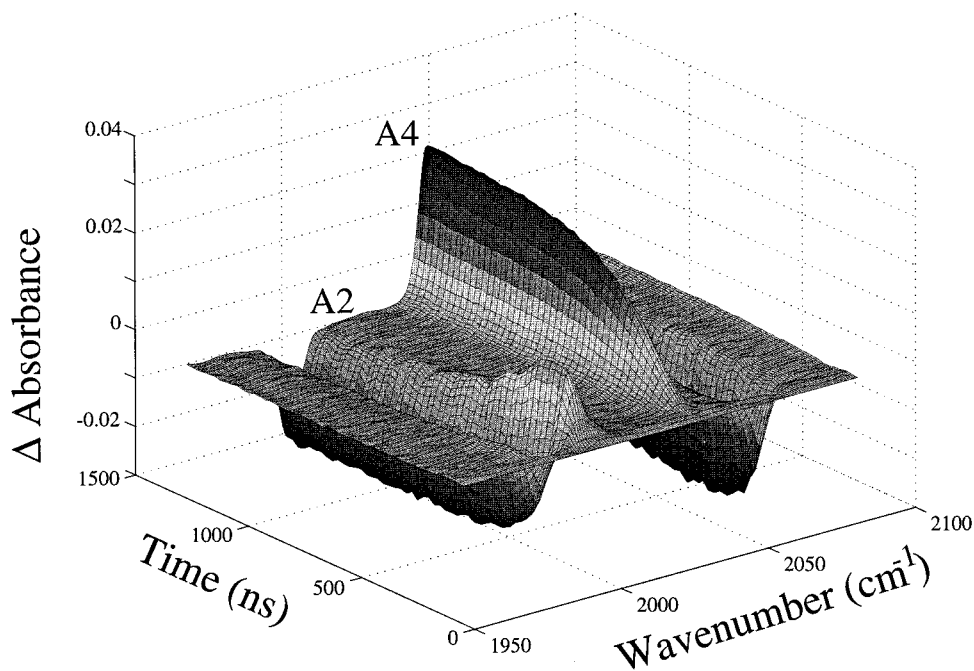


FIGURE 3. Nanosecond spectral evolution of  $\text{Tp}^*\text{Rh}(\text{CO})_2$  in cyclohexane.

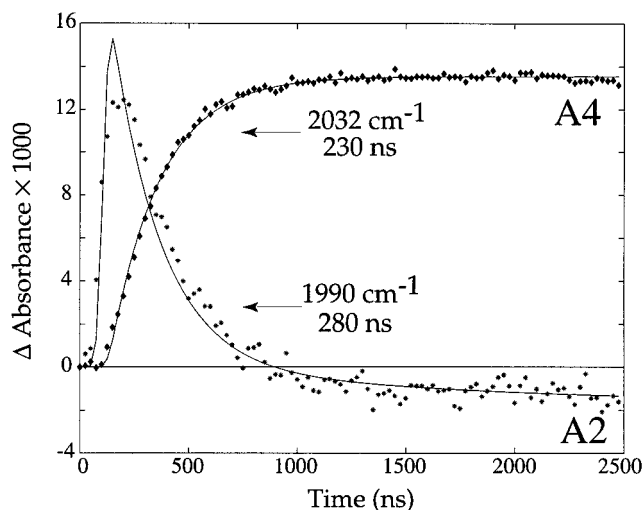


FIGURE 4. Nanosecond kinetics of intermediate **A2** and final alkyl hydride products in cyclohexane.

on the millisecond time scale. Interestingly, no new absorptions are observed in this region of the IR spectrum during the time scales measured. This means that no C–H-activated product forms for the  $\text{Bp}^*\text{Rh}(\text{CO})_2$  chemical system.

Measurement of the time scale  $\tau$  for the last step in the reaction allows an estimate of the free energy barrier for the C–H activation step. Assume that, for these reactions, the reaction rate  $k$  can be modeled as

$$k = \frac{k_b T}{h} \exp\left(-\frac{\Delta G^\ddagger}{RT}\right) \quad (1)$$

where  $k = 1/\tau$ ,  $k_b$  is Boltzmann's constant,  $h$  is Planck's constant,  $R$  is the universal gas constant,  $T$  is the temperature in Kelvin, and  $\Delta G^\ddagger$  is the free energy of the reaction barrier. Using this equation, it is calculated that

the barrier for the dechelation step is 4.2 kcal/mol and for the C–H bond-breaking step the barrier is 8.3 kcal/mol. This 8.3 kcal/mol barrier is significantly less than the 100 kcal/mol C–H bond strength and shows the importance of the metal center in catalyzing this reaction.

A complete diagram of the mechanism for C–H bond activation in the  $\text{Tp}^*\text{Rh}(\text{CO})_2$  system is shown in Figure 5. The dicarbonyl is initially photoexcited, losing one CO ligand. This coordinatively unsaturated (16-electron) molecule forms a solvent complex in a barrierless reaction which takes less than 2 ps. This species is formed with significant excess vibrational energy, which is transferred into the solvent over a time scale of 23 ps. After 200 ps, the complex undergoes a thermal reaction which breaks one of the Rh–N bonds to form the  $\eta^2\text{-Tp}^*\text{Rh}(\text{CO})(\text{S})$  complex with a barrier of  $\sim 4.2$  kcal/mol. This species is the one in which final activation occurs; it crosses a barrier of  $\sim 8.3$  kcal/mol with a time constant of 230 ns to form the fully activated complex, and then the Rh–N bond is reformed to make the final  $\eta^3\text{-Tp}^*\text{Rh}(\text{CO})(\text{H})(\text{R})$  alkyl hydride product.

### 3. Activation of Silane Si–H Bonds

A general reaction scheme for silane Si–H bond activation, derived from low-temperature studies of  $\text{CpM}(\text{CO})_3$  in  $\text{Et}_3\text{-SiH}$  ( $\text{Et} = \text{C}_2\text{H}_5$ ), is shown in Figure 6. It has been conventionally assumed that UV irradiation promotes the metal tricarbonyl **B1** to its excited state, expelling one CO ligand along a dissociation channel to become a coordinatively unsaturated metal dicarbonyl **B2**. In a condensed-phase environment, the vacant coordination site in complex **B2** left behind by the leaving CO ligand is rapidly occupied by a solvent molecule to give a solvated metal dicarbonyl **B3**. The reactive metal center, now shielded by the complexed solvent molecule, can only activate a

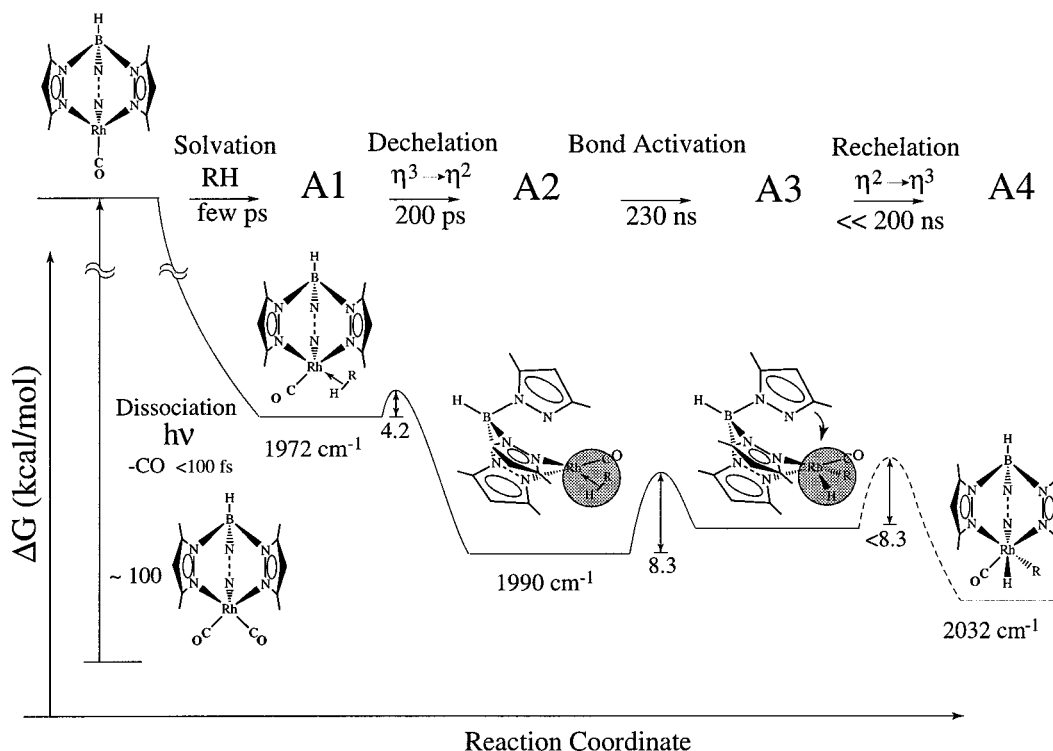


FIGURE 5. Reaction scheme for C–H activation by  $\text{Tp}^*\text{Rh}(\text{CO})_2$ .

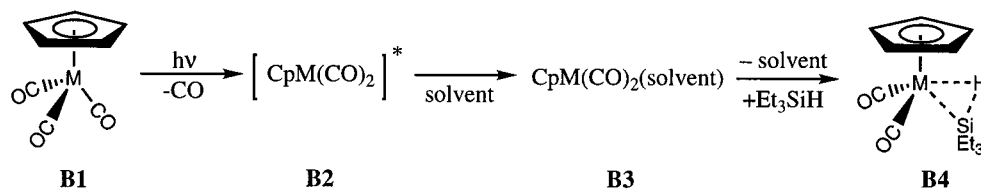


FIGURE 6. Schematic representation of silane Si–H bond activation by  $\text{CpM}(\text{CO})_3$  ( $M = \text{Mn}, \text{Re}$ ).

Si–H bond to form the product **B4** when they interact directly, through displacement of the complexed solvent molecule. This solvent displacement constitutes the apparent rate-determining step of the reaction.<sup>1,15,32–37</sup> In contrast to C–H bond activation, cleavage of a Si–H bond by  $\text{CpRh}(\text{CO})$  has been theoretically shown to be a barrierless reaction.<sup>38,39</sup> Therefore, the time scale of the bond-breaking step is expected to be on the same order as that of the aforementioned solvent complexation, i.e., a few picoseconds in room-temperature solutions.<sup>27</sup>

To assess the activation time scale of a Si–H bond, and thereby the magnitude of the energy barrier which determines it, a reaction scheme composed of elementary reaction steps is needed. Through combined use of femtosecond to nanosecond UV-pump IR-probe spectroscopy and ab initio quantum mechanical calculations, comprehensive reaction mechanisms for reactions of triethylsilane ( $\text{Et}_3\text{SiH}$ ) with  $\text{CpRe}(\text{CO})_3$  and  $\text{CpMn}(\text{CO})_3$  have been derived, as shown in Figures 7 and 8, respectively. Information about the time scale of breaking a Si–H bond was obtained by monitoring the product  $\text{CpM}(\text{CO})_2\text{-(H)(SiEt}_3)$  ( $M = \text{Mn}$  or  $\text{Re}$ ) in the ultrafast regime. Analysis of the product kinetic trace reveals that the formation time of the final product is about 4.4 ps, suggesting that the Si–H bond activation step involves a very small energy barrier, if any.

**3.1. Initial Solvation and Reaction Pathways.** Although the reaction involving the Mn compound appears very complicated compared to that of the Re compound, the two reactions share a common pattern. The newly formed metal dicarbonyls  $\text{CpM}(\text{CO})_2$  resulting from photodissociation of a CO ligand are quickly complexed with a solvent molecule either through the Si–H bond to form the final product on the ultrafast time scale or through an ethyl group to form a reactive intermediate which further reacts to form the final product on a longer (nanosecond to microsecond) time scale. The ethyl solvate, which results from interaction of a metal center with an ethyl group of  $\text{Et}_3\text{SiH}$ , can also be viewed as a kinetically favored intermediate whose relative abundance is expected to be governed by steric interaction.

To study the underlying chemistry, the branching ratios of the two solvation schemes in the reactions of  $\text{CpMn}(\text{CO})_3$  and  $\text{CpRe}(\text{CO})_3$  with  $\text{Et}_3\text{SiH}$  are compared. The branching ratio is derived from kinetic traces of the final product **B13** measured in the nanosecond regime shown in Figure 9. The kinetic trace exhibits an instrument-limited rise due to initial solvation through the Si–H bond on the ultrafast time scale, and an exponential rise due to dissociative rearrangement from alkyl solvate **B12**. The kinetics can be modeled using the following equation:

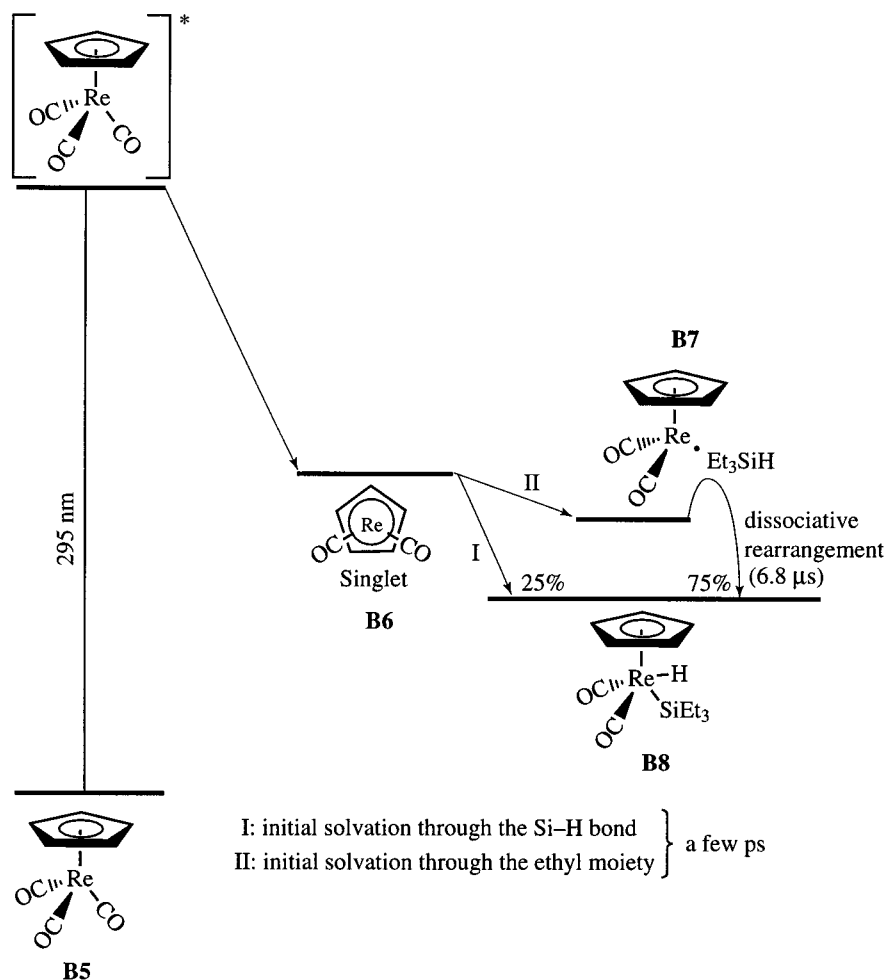


FIGURE 7. Proposed reaction mechanism of silane Si-H bond activation by  $\text{CpRe}(\text{CO})_3$  (compound **B5**).

where  $I(t)$  is the intensity of the observed transient species,  $C_0$  and  $C_1$  are constants proportional to the probability of solvation through the Si-H bond and that of solvation through the ethyl moiety, respectively, and  $\tau$  is the time constant for the rearrangement process. The ratios  $C_1/C_0$  for the Mn and Re complexes are found to be 5.3 and 3, respectively. These results indicate that because of its larger diameter and consequently reduced steric hindrance, the Re center of a  $\text{CpRe}(\text{CO})_2$  samples equivalently the three ethyl groups and single Si-H bond in an  $\text{Et}_3\text{SiH}$  molecule during initial solvation, while the Mn center does not.

### 3.2. Electronic Configuration and Reaction Pathways.

One turns next to the differences in reaction mechanisms involving Mn and Re atoms. Although Mn and Re belong to the same group in the periodic table, their reactivity toward activating a Si-H bond depends critically on the electronic structure of the organometallic complexes. Promotion of a parent molecule to different regions of the electronically excited manifold may lead to dissociation channels that result in dicarbonyls of different morphology and/or electronic multiplicity. This aspect of reactivity is demonstrated in the reaction of the manganese complex with  $\text{Et}_3\text{SiH}$ .

Figure 10 shows the transient difference infrared spectra taken at -10, 10, 33, 200, and 660 ps time delays

with respect to the UV excitation pulse. The last panel is a static FTIR spectrum for the purpose of comparison. In the 10 ps panel, the two bands at 1892 and 1960  $\text{cm}^{-1}$  are due to an ethyl solvate **B12**, resulting from solvation of singlet  $\text{CpMn}(\text{CO})_2$ , labeled **B10**, through the ethyl moiety of a solvent molecule. Bands at 1883 and 2002  $\text{cm}^{-1}$  which also appear in the 10 ps panel are attributed to  $\text{CpMn}(\text{CO})_2$  in its triplet state, labeled **B11**, according to results from ab initio calculations. Species **B12** is more energetically stable than **B11**, the latter decaying to the former within 200 ps as shown in Figure 10. These two dicarbonyl intermediates can be considered as emerging from two parallel channels that are governed by dynamic partitioning processes determined by the excited potential energy surface of  $\text{CpMn}(\text{CO})_3$ . As shown in the inset of Figure 8, there are two distinct electronic excited states accessible under the present experimental conditions. Both excited states are expected to be populated when a sample of  $\text{CpMn}(\text{CO})_3$  is irradiated with UV light because there is substantial overlap between the two electronic bands. This explains why both singlet and triplet dicarbonyls were observed.

The correlations between the excited states and the observed intermediates were studied by comparing the relative abundance, or branching ratio, of **B12** and **B11** when subjected to different excitation energies. The

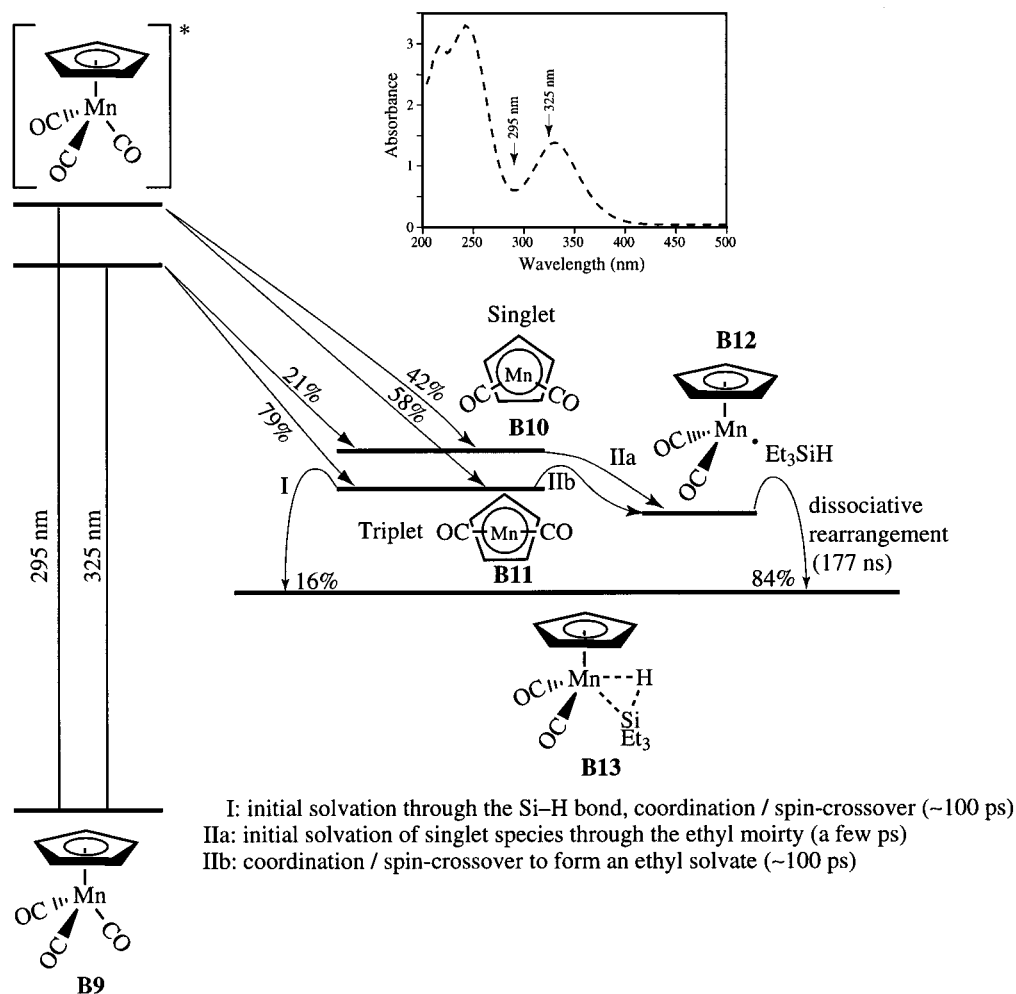


**FIGURE 8.** Proposed reaction mechanism of silane Si-H bond activation by  $\text{CpMn(CO)}_3$  (compound **B9**). Inset: UV-vis spectrum of  $\text{CpMn(CO)}_3$  in neat  $\text{Et}_3\text{SiH}$  under experimental conditions. Arrows indicate the excitation wavelengths used in the present studies.

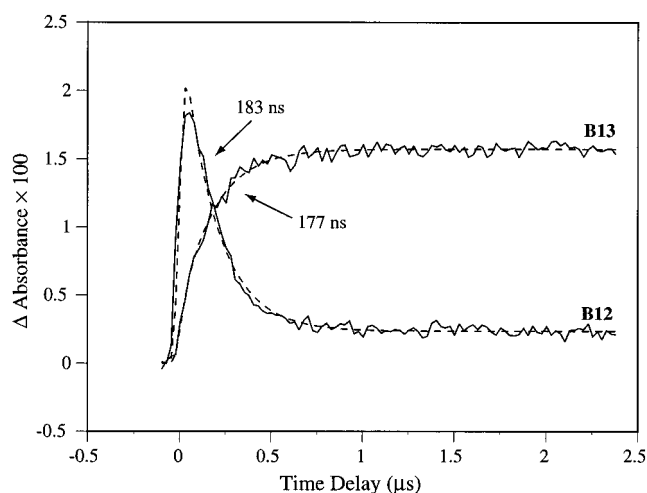


**FIGURE 9.** Time-resolved step-scan FTIR kinetic traces showing the rise of the product **B13** and decay of the alkyl-solvated intermediate **B12**. Also shown are the corresponding single-exponential fit (dashed lines) and time constants.

$$I(t) = C_0 + C_1 e^{-t/\tau} \quad (2)$$

branching ratios of **B12** to **B11**, derived from kinetic studies of **B12**, are found to be 1:1 for 295 nm excitation

and 1:3 for 325 nm excitation. The lower-energy band peaking at about 330 nm is therefore correlated with formation of  $\text{CpMn(CO)}_2$  in its triplet state, whereas the higher-energy band (<295 nm) is correlated with formation of  $\text{CpMn(CO)}_2$  in its singlet state.

**3.3. Nature of the Silane Intermediates.** Typically, the energy required to break a transition-metal-CO bond is about 45–50 kcal/mol.<sup>40</sup> The energy carried by a 295 or 325 nm laser beam is equivalent to 97 or 88 kcal/mol, respectively. With these numbers in mind, the nascent metal dicarbonyl resulting from the loss of a CO ligand would have to deposit to its environment at least ~40 kcal/mol of energy before forming an observable intermediate. It is conceivable that the metal complex may experience changes in molecular conformation and/or electronic multiplicity during the energy dissipation process. The observed intermediates were studied using ab initio calculations because the lifetimes of those transient species are often too short for conventional characterization techniques such as nuclear magnetic resonance (NMR) and electron spin resonance (ESR).

The optimized molecular geometry of  $\text{CpMn(CO)}_2 \cdot (\text{H}_3\text{CCH}_3)$  (representing species **B12**) and that of **B11** are shown at the top and bottom, respectively, of Figure 11.

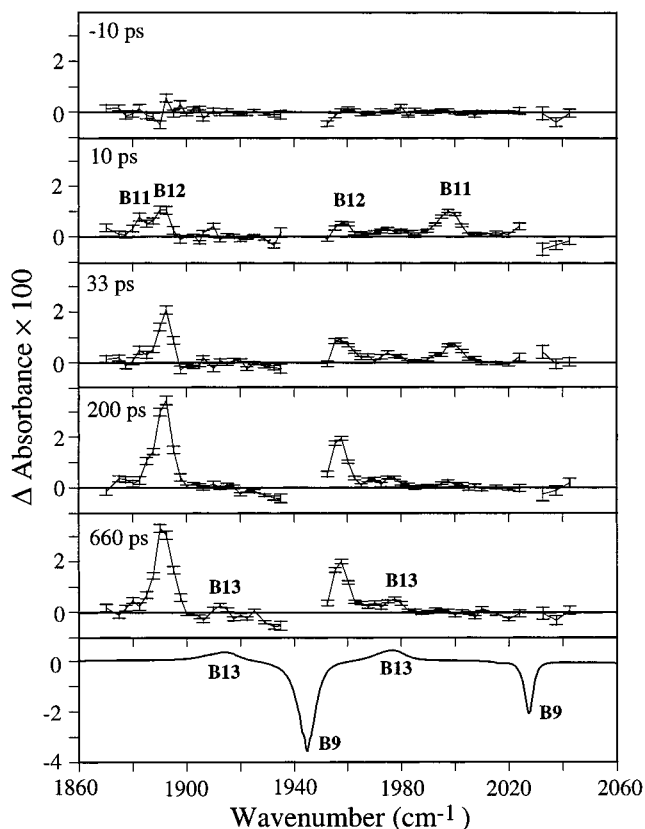


**FIGURE 10.** Transient difference spectra in the CO stretching region for  $\text{CpMn(CO)}_3$  in neat triethylsilane at  $-10$ ,  $10$ ,  $33$ ,  $200$ , and  $660$  ps following  $325$  nm UV photolysis. Under the experimental conditions, the large cross-sections of the solvent Si–H band ( $\sim 2100$   $\text{cm}^{-1}$ ) and the parent CO bands ( $1947$  and  $2028$   $\text{cm}^{-1}$ ) make it difficult to access some regions of the spectrum. The last panel is a static FTIR difference spectrum before and after UV photolysis at  $308$  nm.

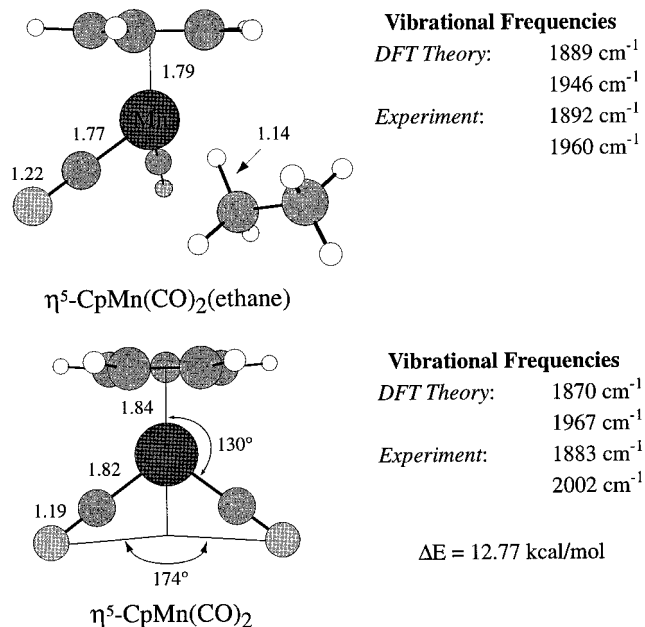


**FIGURE 11.** Geometries of  $\text{CpMn(CO)}_2(\text{H}_3\text{CCH}_3)$  and  $\text{CpMn(CO)}_2$  in the electronic triplet state. Both are optimized at the MP2/lan12dz level of theory. Bond lengths are in angstroms and angles in degrees.

Also shown are some key parameters, including their relative energies, bond angles, bond lengths, and calcu-

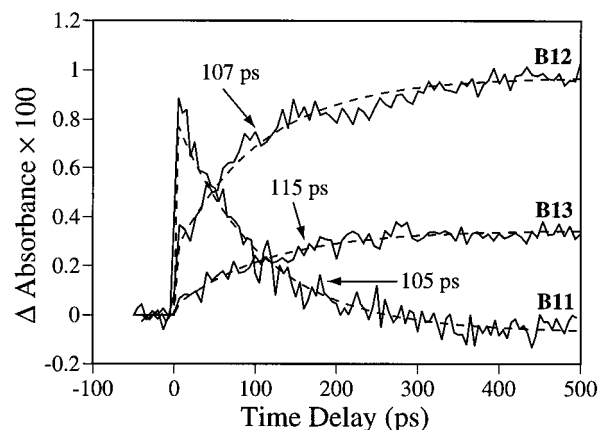


**FIGURE 12.** Ultrafast kinetics (solid lines) of  $\text{CpMn(CO)}_3$  in neat triethylsilane after  $325$  nm UV photolysis at  $1979$   $\text{cm}^{-1}$  (Figure 10, **B13**) and the CO stretch of the silyl adduct  $\text{CpMn(CO)}_2(\text{H})(\text{SiEt}_3)$ ,  $2002$   $\text{cm}^{-1}$  (Figure 10, **B11**),  $1892$   $\text{cm}^{-1}$  (Figure 10, **B12**). The frequencies were chosen to minimize overlap with adjacent peaks. Time constants for the exponential fits (dashed lines) are shown in the figure.

lated vibrational frequencies. Qualitative understanding of steric interactions can be deduced from these geometric parameters. In addition, because IR bands have better spectral resolution than UV–vis bands, ab initio vibrational frequencies are helpful in assigning identities to transient intermediates, as in the case of the manganese complex. Results from such calculations also provide insights into the nature of the interactions between a metal complex and solvent molecules. A growing body of evidence has shown that transition-metal complexes of triplet character interact weakly with, or are slightly solvated by, weakly binding ligands such as alkanes and inert gas molecules. The interaction with strongly binding ligands including CO, C=C, and Si–H bonds, however, may be sufficiently strong to cause a presumably concerted spin-crossover/coordination process.<sup>7,20,41–44</sup> As a consequence, it would appear that triplet  $\text{CpMn(CO)}_2$  tends to be preferentially solvated through the Si–H bond of  $\text{Et}_3\text{SiH}$  to form singlet  $\text{CpMn(CO)}_2(\text{H})(\text{SiEt}_3)$ , whereas the singlet  $\text{CpMn(CO)}_2$  gives little contribution to the formation of the final product in the ultrafast regime. This is evidenced by the single-exponential rise of the product kinetics shown in Figure 12.

## 4. Conclusions

Time-resolved infrared spectroscopy, which provides both structural and temporal information concerning a chemical system, has been instrumental in understanding chemical reactions by identifying and monitoring the reactive intermediates. The vibrational modes of a molecule are determined by its chemical environment, its morphology, and its electronic structure. In particular, the CO stretch of a metal carbonyl carries information about the electron density and chemical bonding at the metal center. The use of time-resolved infrared spectroscopy has allowed for the detailed study of organometallic reaction systems. Reaction mechanisms have been studied for both C–H and Si–H bond activation. Both reactions proceed



through extremely reactive coordinatively unsaturated intermediates, forming solvent complexes within picoseconds, and then undergo vibrational cooling.

In the case of C–H activation, it was established that, for  $\text{Cp}^*\text{Rh}(\text{CO})_2$ , the quantum yield is a function of the partition between a CO dissociative state and a nondissociative excited electronic state. Studies of C–H activation by  $\text{Tp}^*\text{Rh}(\text{CO})_2$  show that the time scale for final C–H activation is  $\sim 200$  ns for cyclic hydrocarbons, suggesting a barrier of 8.3 kcal/mol for the bond-breaking step.  $\text{Tp}^*\text{Rh}(\text{CO})_2$  also shows interesting dynamics as a function of ligand connectivity at the metal center. At 200 ps after photoexcitation, the ligand partially dechelates to form the  $\eta^2\text{-Tp}^*\text{Rh}(\text{H})(\text{S})$  complex. Reaction to form the final alkyl hydride occurs from this state, and involves the breaking of the C–H bond, followed by re-formation of the Rh–N bond.

For Si–H activation, markedly different behavior was observed. The reaction in  $\text{CpRe}(\text{CO})_3$  is partitioned into two distinct channels upon initial photoexcitation. These channels represent coordination of the dicarbonyl intermediate through the Si–H bond or through an ethyl moiety of the solvent molecule. Activation of the Si–H complex occurs in a few picoseconds, while activation of the ethyl complex occurs on a much longer time scale of 6.8  $\mu\text{s}$ . The longer activation time of the ethyl complex suggests that rearrangement proceeds via a dissociative rearrangement mechanism. In  $\text{CpMn}(\text{CO})_3$  the reaction is similar, but there exist two initially formed excited electronic states. This leads to two possible intermediates (singlet or triplet), each with two associated reaction pathways (solvation through the Si–H bond or through the ethyl moiety). Thus, the course of the reaction is determined by the initially formed excited state and by the initial solvation process.

These studies have shown that it is possible to study very complex bimolecular chemical reactions to produce a detailed picture of the mechanisms involved in the reactions. These studies have also shown that reaction steps which occur on the ultrafast time scale, such as structural change, electronic state partitioning, and solvation, can have a dramatic effect on reactivity on a much longer time scale. It is expected that time-resolved infrared spectroscopy, especially in the ultrafast regime, will find wide application in the studies of bimolecular reactions. The information thus obtained will be helpful in the construction of reaction coordinates of complex reactions, which has been a challenge in understanding the processes of chemical reactions in condensed phases at the molecular level.

We thank Professors R. G. Bergman and C. B. Moore and Dr. H. Frei for fruitful discussions of the present work and Dr. B. K. McNamara and Mr. J. S. Yeston for their assistance in sample preparation. The use of the Bruker IFS88 FTIR spectrophotometer in Dr. Frei's laboratory is gratefully acknowledged. This work was supported by a grant from the National Science Foundation.

## References

- (1) Jetz, W.; Graham, W. A. G. Silicon-Transition Metal Chemistry. I. Photochemical Preparation of Silyl-(transition metal) Hydrides. *Inorg. Chem.* **1971**, *10*, 4–9.
- (2) Janowicz, A. H.; Bergman, R. G. C–H Activation in Completely Saturated Hydrocarbons: Direct Observation of  $\text{M} + \text{R-H} \rightarrow \text{M}(\text{R})(\text{H})$ . *J. Am. Chem. Soc.* **1982**, *104*, 352–355.
- (3) Bergman, R. G. Activation of Alkanes with Organotransition Metal Complexes. *Science* **1984**, *223*, 902–908.
- (4) Hoyano, J. K.; Graham, W. A. G. Oxidative Addition of the Carbon–Hydrogen Bonds of Neopentane and Cyclohexane to a Photochemically Generated Iridium(I) Complex. *J. Am. Chem. Soc.* **1982**, *104*, 3723–3725.
- (5) Wasserman, E. P.; Moore, C. B.; Bergman, R. G. Gas-Phase Rates of Alkane C–H Oxidative Addition to a Transient  $\text{CpRh}(\text{CO})$  Complex. *Science* **1992**, *255*, 315–318.
- (6) Bengali, A. A.; Schultz, R. H.; Moore, C. B.; Bergman, R. G. Activation of the C–H Bonds in Neopentane and Neopentane- $\text{D}_{12}$  by  $(\eta^5\text{-C}_5(\text{CH}_3)_5)\text{Rh}(\text{CO})_2$ —Spectroscopic and Temporal Resolution of Rhodium–Krypton and Rhodium–Alkane Complex Intermediates. *J. Am. Chem. Soc.* **1994**, *116*, 9585–9589.
- (7) Bengali, A. A.; Bergman, R. G.; Moore, C. B. Evidence for the Formation of Free 16-Electron Species Rather than Solvate Complexes in the Ultraviolet Irradiation of  $\text{CpCo}(\text{CO})_2$  in Liquefied Noble Gas Solvents. *J. Am. Chem. Soc.* **1995**, *117*, 3879–3880.
- (8) Perutz, R. N.; Belt, S. T.; McCamley, A.; Whittlesey, M. K. C–H Activation by Organometallics—The Role of Matrix Isolation Studies. *Pure Appl. Chem.* **1990**, *62*, 1539–1545.
- (9) Bloyce, P. E.; Mascetti, J.; Rest, A. J. Photochemistry of *tris*(Dimethylpyrazolyl)-boratorhodium Dicarbonyl and *bis*(Dimethylpyrazolyl)-boratorhodium Dicarbonyl Complexes in Low Temperature Media at 12–298 K—Some insights into C–H Activation Processes. *J. Organomet. Chem.* **1993**, *444*, 223–233.
- (10) Pradella, F.; Rehorek, D.; Scoconi, M.; Sostero, S.; Traverso, O. Matrix and Solution Photochemistry of  $[\text{C}_5(\text{CH}_3)_5\text{Rh}(\text{CO})_2]$ . *J. Organomet. Chem.* **1993**, *453*, 283–288.
- (11) Bromberg, S. E.; Lian, T. Q.; Bergman, R. G.; Harris, C. B. Ultrafast Dynamics of  $\text{Cp}^*\text{M}(\text{CO})_2$  ( $\text{M} = \text{Ir}, \text{Rh}$ ) in Solution—The Origin of the Low Quantum Yields for C–H Bond Activation. *J. Am. Chem. Soc.* **1996**, *118*, 2069–2072.
- (12) Bromberg, S. E.; Yang, H.; Asplund, M. C.; Lian, T.; McNamara, B. K.; Kotz, K. T.; Yeston, J. S.; Wilkens, M.; Frei, H.; Bergman, R. G.; Harris, C. B. The Mechanism of a C–H Bond Activation Reaction in Room-Temperature Alkane Solution. *Science* **1997**, *278*, 260–263.
- (13) Lian, T.; Bromberg, S. E.; Yang, H.; Proulx, G.; Bergman, R. G.; Harris, C. B. Femtosecond IR Studies of Alkane C–H Bond Activation by Organometallic Compounds—Direct Observation of Reactive Intermediates in Room Temperature Solutions. *J. Am. Chem. Soc.* **1996**, *118*, 3769–3770.
- (14) Yang, H.; Kotz, K. T.; Asplund, M. C.; Harris, C. B. Femtosecond Infrared Studies of Silane Silicon–Hydrogen Bond Activation. *J. Am. Chem. Soc.* **1997**, *119*, 9564–9565.

- (15) Yang, H.; Asplund, M. C.; Kotz, K. T.; Wilkens, M. J.; Harris, C. B.; Frei, H. Reaction Mechanism of Silicon-Hydrogen Bond Activation Studied Using Femtosecond to Nanosecond Spectroscopy and Ab Initio Methods. *J. Am. Chem. Soc.* **1998**, *120*, 10154–10165.
- (16) Lian, T. Q.; Bromberg, S. E.; Asplund, M. C.; Yang, H.; Harris, C. B. Femtosecond Infrared Studies of the Dissociation and Dynamics of Transition Metal Carbonyls in Solution. *J. Phys. Chem.* **1996**, *100*, 11994–12001.
- (17) Sun, H.; Frei, H. Time-Resolved Step-Scan Fourier Transform Infrared Spectroscopy of Triplet Excited Duroquinone in a Zeolite. *J. Phys. Chem. B* **1997**, *101*, 205–209.
- (18) Weiller, B. H.; Wasserman, E. P.; Moore, C. B.; Bergman, R. G. Organometallic CO Substitution Kinetics in Liquid Xe by Fast Time-Resolved IR Spectroscopy. *J. Am. Chem. Soc.* **1993**, *115*, 4326–4330.
- (19) Marx, D.; Lees, A. J. Photochemistry of Dicarbonyl- $(\eta^5\text{-Cyclopentadienyl})$ Iridium in Hydrocarbon Solutions—Kinetics and Mechanism of C–H Bond Activation. *Inorg. Chem.* **1988**, *27*, 1121–1122.
- (20) Dougherty, T. P.; Heilweil, E. J. Transient Infrared Spectroscopy of  $(\eta^5\text{-C}_5\text{H}_5)\text{Co}(\text{CO})_2$  Photoproduct Reactions in Hydrocarbon Solutions. *J. Chem. Phys.* **1994**, *100*, 4006–4009.
- (21) Ghosh, C. K.; Graham, A. G. Efficient and Selective Carbon-Hydrogen Activation by a *tris*(Pyrazolyl)borate Rhodium Complex. *J. Am. Chem. Soc.* **1987**, *109*, 4726–4727.
- (22) Ghosh, C. K.; Graham, A. G. A Rhodium Complex that Combines Benzene Activation with Ethylene Insertion—Subsequent Carbonylation and Ketone Formation. *J. Am. Chem. Soc.* **1989**, *111*, 375–376.
- (23) Lees, A. J.; Purwoko, A. A. Photochemical Mechanisms in Intermolecular C–H Bond Activation Reactions of Organometallic Complexes. *Coord. Chem. Rev.* **1994**, *132*, 155–160.
- (24) Purwoko, A. A.; Lees, A. J. Photochemistry and C–H Bond Activation Reactivity of  $(\text{HBPz}^*)\text{Rh}(\text{CO})_2$  ( $\text{Pz}^* = 3,5\text{-Dimethylpyrazolyl}$ ) in Hydrocarbon Solution. *Inorg. Chem.* **1995**, *34*, 424–425.
- (25) Tro, N. J.; King, J. C.; Harris, C. B. Ultrafast Studies of Metal–Metal Bond Cleavage in  $\text{Fe}_3(\text{CO})_{12}$  in Solution. *Inorg. Chim. Acta* **1995**, *229*, 469–471.
- (26) Beckerle, J. D.; Casassa, M. P.; Cavanagh, R. R.; Heilweil, E. J.; Stephensen, J. C. Sub-Picosecond Time-Resolved IR Spectroscopy of the Vibrational Dynamics of  $\text{Rh}(\text{CO})_2(\text{Acac})$ . *Chem. Phys.* **1992**, *160*, 487–497.
- (27) King, J. C.; Zhang, J. Z.; Schwartz, B. J.; Harris, C. B. Vibrational Relaxation of  $\text{M}(\text{CO})_6$  ( $\text{M} = \text{Cr}, \text{Mo}, \text{W}$ )—Effect of Metal Mass on Vibrational Cooling Dynamics and Non-Boltzmann Internal Energy. *J. Chem. Phys.* **1993**, *99*, 7595–7601.
- (28) Lee, M.; Harris, C. B. Ultrafast Studies of Transition-Metal Carbonyl Reactions in the Condensed Phase—Solvation of Coordinatively Unsaturated Pentacarbonyls. *J. Am. Chem. Soc.* **1989**, *111*, 8963–8965.
- (29) Xu, X. B.; Lingle, R.; Yu, S. C.; Chang, Y. J.; Hopkins, J. B. Direct Measurement of Photodissociation, Geminate Recombination, and Vibrational Cooling in Iodine Using Picosecond Raman Spectroscopy. *J. Chem. Phys.* **1990**, *92*, 2106–2107.
- (30) Wick, D. D.; Goldberg, K. I. C–H Activation at Pt(II) To Form Stable Pt(IV) Alkyl Hydrides. *J. Am. Chem. Soc.* **1997**, *119*, 10235–10236.
- (31) Zanic, S.; Hall, M. B. Prediction of the Reactive Intermediates in Alkane Activation by *tris*(pyrazolyl)-rhodium carbonyl. *J. Phys. Chem. A* **1998**, *102*, 1963–64.
- (32) Wrighton, M. S.; Schroeder, M. A. Chromium Carbonyl Photocatalyzed 1,4-Hydrosilylation of 1,3 Dienes. A Synthesis of Allylsilanes. *J. Am. Chem. Soc.* **1974**, *96*, 6235–6237.
- (33) Schubert, U.  $\eta^2$  Coordination of Si–H  $\sigma$  Bonds to Transition Metals. *Adv. Organomet. Chem.* **1990**, *30*, 151–187.
- (34) Young, K. M.; Wrighton, M. S. Temperature-Dependence of the Oxidative Addition of Triethylsilane to Photochemically Generated  $(\eta^5\text{-C}_5\text{Cl}_5)\text{Mn}(\text{CO})_2$ . *Organometallics* **1989**, *8*, 1063–1066.
- (35) Hart-Davis, A. J.; Graham, W. A. G. Silicon-Transition Metal Chemistry. VI. Kinetics and Mechanism of the Replacement of Triphenylsilane by Triphenylphosphine in Hydridotriphenylsilyl( $\tau$ -cyclopentadienyl)dicarbonylmanganese. *J. Am. Chem. Soc.* **1971**, *93*, 4388–4393.
- (36) Hill, R. H.; Wrighton, M. S. Oxidative Addition of Trisubstituted Silanes to Photochemically Generated Coordinatively Unsaturated Species  $(\eta^4\text{-C}_4\text{H}_4)\text{-Fe}(\text{CO})_2$ ,  $(\eta^5\text{-C}_5\text{H}_5)\text{Mn}(\text{CO})_2$ , and  $(\eta^6\text{-C}_6\text{H}_6)\text{Cr}(\text{CO})_2$  and Related Molecules. *Organometallics* **1987**, *6*, 632–638.
- (37) Palmer, B. J.; Hill, R. H. The Energetics of the Oxidative Addition of Trisubstituted Silanes to Photochemically Generated  $(\eta^5\text{-C}_5\text{H}_5)\text{Mn}(\text{CO})_2$ . *Can. J. Chem.* **1996**, *74*, 1959–1967.
- (38) Koga, N.; Morokuma, K. SiH, SiSi, and CH Bond Activation by Coordinatively Unsaturated  $\text{RhCl}(\text{PH}_3)_2$ —Ab Initio Molecular Orbital Study. *J. Am. Chem. Soc.* **1993**, *115*, 6883–6892.
- (39) Musaev, D. G.; Morokuma, K. Ab Initio Molecular Orbital Study of the Mechanism of H–H, C–H, N–H, O–H, and Si–H Bond Activation on Transient Cyclopentadienylcarbonylrhodium. *J. Am. Chem. Soc.* **1995**, *117*, 799–805.
- (40) Klassen, J. K.; Selke, M.; Sorensen, A. A.; Yang, G. K. Metal–Ligand Bond Dissociation Energies in  $\text{CpMn}(\text{CO})_2\text{L}$  Complexes. *J. Am. Chem. Soc.* **1990**, *112*, 1267–1268.
- (41) Blomberg, M. R. A.; Siegbahn, P. E. M.; Svensson, M. Mechanisms for the Reactions between Methane and the Neutral Transition Metal Atoms from Yttrium to Palladium. *J. Am. Chem. Soc.* **1992**, *114*, 6095–6102.
- (42) Siegbahn, P. E. M.; Svensson, M. Different Electronic Structure Requirements on Precursors and Transition States for the Oxidative Addition Reaction with Methane. *J. Am. Chem. Soc.* **1994**, *116*, 10124–10128.
- (43) Carroll, J. J.; Weisshaar, J. C.; Huag, K. L.; Blomberg, M. R. A.; Siegbahn, P. E. M.; Svensson, M. Gas Phase Reactions of Second-Row Transition Metal Atoms with Small Hydrocarbons—Experiment and Theory. *J. Phys. Chem.* **1995**, *99*, 13955–13969.
- (44) Siegbahn, P. E. M. Comparison of the C–H Activation of Methane by  $\text{M}(\text{C}_5\text{H}_5)(\text{CO})$  for  $\text{M} = \text{Cobalt}, \text{Rhodium}, \text{and Iridium}$ . *J. Am. Chem. Soc.* **1996**, *118*, 1487–1496.

AR970133Y